

Time- and space-resolved selective multipair creation

Q. Z. Lv* and Heiko Bauke†

Max-Planck-Institut für Kernphysik, Saupfercheckweg 1, 69117 Heidelberg, Germany

(Dated: October 1, 2018)

The simultaneous creation of multiple electron-positron pairs by localized strong electric fields is studied by utilizing a time- and space-resolved quantum field theory approach. It is demonstrated that the number of simultaneously created pairs equals the number of the potential's supercritical quasibound states in the Dirac sea. This means it can be controlled by tuning the potential parameters. Furthermore, the energy of the created particles corresponds to the energy of the supercritical quasibound states. The simultaneously created electrons and positrons are statistically correlated, which is reflected in the spatial distribution and the momentum distribution of these particles and antiparticles.

PACS numbers: 34.50.Rk, 03.65.-w, 42.50.-p

1. Introduction

The vacuum is the lowest energy eigenstate of the field-free quantum field Hamiltonian. In the presence of a strong external field this state, however, may become instable. This leads to the spontaneous emission of electron-positron pairs, which is one of the most striking predictions of the Dirac equation in its quantum field theoretical formulation [1]. While early predictions of this possibility date back to Heisenberg and Euler [2], Sauter [3] and others in the early part of the past century, the first calculation of the pair-production rate based on a nonperturbative approach was accomplished by Schwinger [4] in the early 1950s.

Using Schwinger's formula, one finds that a sizable pair-creation rate requires an electric field of the strength $E_{\text{cr}} = m_e c^2 / e = 1.3 \times 10^{18}$ V/m, which is very difficult to produce in the laboratory. Here m_e , e , and c denote the electron mass, the elementary charge, and the speed of light. Further studies [5, 6] extended Schwinger's pioneering work to calculate the long-time pair-creation behavior for spatially inhomogeneous electric fields. Several investigations involving the combination of different static electric, magnetic, and time-dependent laser fields [7–10] suggest that pair creation may be realized below the Schwinger critical field strength E_{cr} .

In theoretical terms, the breakdown of the vacuum is associated with a depopulation of states in the initially filled negative-energy Dirac sea. In Ref. [11], it was suggested that quasibound states that are embedded in the negative-energy continuum may be solely responsible for pair creation. If the charge of a combined nucleus is so large that the energies of the lowest lying bound states drift below $-m_e c^2$, these states can dive into the negative energy continuum and trigger pair creation. Recently, several works [12–14] have also argued that discrete states can act as a transfer channel for population between the positive-energy and negative-energy states and thus enhance the creation rate.

In fact, starting in the early 1980s heavy ion collision experiments [15, 16] were performed with the hope that the combined

Coulomb field of two colliding nuclei would be sufficient to break down the vacuum [17] and to produce electron-positron pairs. However, the observed positrons can also be caused by the presence of the unavoidable transitions associated with the internal nuclear structure and not triggered by the Coulomb field alone. There is also the prospect that future focused laser pulses could provide sufficiently large fields to trigger the purely spontaneous creation of particle pairs from the vacuum.

In recent years, quantum control has become a mature and active research field which deals with the active manipulation of physical processes on the quantum level [18]. Usually sophisticated schemes are required to drive a quantum system into a specific desired final state. It is well known that tuning the parameters of the binding potential can be utilized to control the *average* number of created pairs [19, 20]. However, it remains unknown to which field states these pairs actually belong. For example, an expectation value for the number of created pairs of one can correspond to a system that is definitely in a single-pair state. The same count can, however, also characterize a different state that is an equal-weight superposition of the vacuum and a two-pairs state. Furthermore, to the best of our knowledge there is also no method to control a quantum system such that it evolves into a certain field state during the pair-creation dynamics. Both issues will be addressed in this article, which focuses on the pair production caused by a strong external binding potential.

In this contribution we employ a quantum field theoretical description of the pair-creation dynamics to study the creation of single-pair states, two-pair states, and so on. The numerical time-dependent solution of the corresponding theoretical equations on a space-time grid will give us deeper insight than the standard S-matrix approach, which can only represent the system's asymptotic behavior. For example, it allows one to determine the space-resolved densities of multipair states with a given number of electron-positron pairs. We will demonstrate that a strong localized binding potential can be tuned to create selectively multipair states with a specific number of electrons and positrons, e. g., single-pair states or two-pair states.

This paper is organized as follows. In order to render the presentation self-contained, Sec. 2 describes the theoretical framework of numerical time-dependent quantum field theory, which allows us to investigate the field states as well as the

* qingzheng.lyu@mpi-hd.mpg.de

† heiko.bauke@mpi-hd.mpg.de

pair-creation dynamics via arbitrary external force fields. In Sec. 3, we discuss the pair-creation process for fermionic systems induced by a localized binding potential and investigate the spatial and temporal signatures of the final field states. In Sec. 4, we give a brief summary.

2. Theoretical description of the pair-creation dynamics

The creation of particle-antiparticle pairs can be viewed as the vacuum turns into different field states in the Fock space, i. e., the vacuum state, single-pair states, two-pair states etc. All these states are the eigenstates of the field-free quantum field Hamiltonian and can be used as a basis to span the Hilbert space. Starting from the vacuum, the final state of the system is a superposition of several states in this basis. As illustrated

$$\begin{aligned} \|\Omega(t)\rangle\rangle &= c_0(t) \|\text{vac}\rangle\rangle + \\ &c_{1,1}(t) \|e_{p_1,s_1}^+ e_{p'_1,s'_1}^-\rangle\rangle + c_{1,2}(t) \|e_{p_1,s_1}^+ e_{p'_2,s'_2}^-\rangle\rangle + c_{1,3}(t) \|e_{p_2,s_2}^+ e_{p'_1,s'_1}^-\rangle\rangle + \dots \\ &c_{2,1}(t) \|e_{p_1,s_1}^+ e_{p_2,s_2}^+ e_{p'_1,s'_1}^- e_{p'_2,s'_2}^-\rangle\rangle + c_{2,2}(t) \|e_{p_1,s_1}^+ e_{p_3,s_3}^+ e_{p'_1,s'_1}^- e_{p'_2,s'_2}^-\rangle\rangle + c_{2,3}(t) \|e_{p_1,s_1}^+ e_{p_2,s_2}^+ e_{p'_1,s'_1}^- e_{p'_3,s'_3}^-\rangle\rangle + \dots \\ &c_{3,1}(t) \|e_{p_1,s_1}^+ e_{p_2,s_2}^+ e_{p_3,s_3}^+ e_{p'_1,s'_1}^- e_{p'_2,s'_2}^- e_{p'_3,s'_3}^-\rangle\rangle + c_{3,2}(t) \|e_{p_1,s_1}^+ e_{p_2,s_2}^+ e_{p_4,s_4}^+ e_{p'_1,s'_1}^- e_{p'_2,s'_2}^- e_{p'_3,s'_3}^-\rangle\rangle + \dots, \end{aligned} \quad (1)$$

where $\|\text{vac}\rangle\rangle$ denotes the vacuum state, $\|e_{p_1,s_1}^+ e_{p'_1,s'_1}^-\rangle\rangle$ is a single-pair state with an electron (e^+) and a positron (e^-) [25], $\|e_{p_1,s_1}^+ e_{p_2,s_2}^+ e_{p'_1,s'_1}^- e_{p'_2,s'_2}^-\rangle\rangle$ refers a two-pair state and so on. A superposition of multipair states with all of the same number of particle-antiparticle pairs is called a “number state” in the following. Mathematically, a multipair state with n pairs is created from the vacuum state by applying the creation operators $\hat{a}_{p,s}^+$ and $\hat{a}_{p,s}^-$ for the particle and the antiparticle, respectively, on it, i. e.,

$$\|e_{p_1,s_1}^+ \dots e_{p_n,s_n}^+ e_{p'_1,s'_1}^- \dots e_{p'_n,s'_n}^-\rangle\rangle = \prod_{i=1}^n \hat{a}_{p_i,s_i}^+ \hat{a}_{p'_i,s'_i}^- \|\text{vac}\rangle\rangle. \quad (2)$$

The corresponding annihilation operators will be denoted by $\hat{a}_{p,s}^+$ and $\hat{a}_{p,s}^-$. These fermionic annihilation and creation operators satisfy the anticommutator relations

$$\{\hat{a}_{p,s}^+, \hat{a}_{p',s'}^+\} = \{\hat{a}_{p,s}^-, \hat{a}_{p',s'}^-\} = \delta_{p,p'} \delta_{s,s'}, \quad (3)$$

where $\delta_{i,j}$ denotes a Kronecker delta. The amplitudes of these states are represented by $c_0(t)$ for vacuum and $c_{i,j}(t)$ for the j th single- or multipair state containing i electrons and positrons. As the number of ways to combine particle-antiparticle pairs into multipair states grows rapidly with the number of pairs it is not feasible to calculate the amplitudes for all states. Instead, we define various observables based on the quantum field operator to characterize the quantum field state in the following.

The quantum field operator of a fermionic many-particle system can be expressed as an integral or a sum (in the case

below, this quantum field state can be determined by solving the time-dependent Dirac equation for all basis vectors of the corresponding single-particle Hilbert space [21–24]. The number of field states that contain a specific count of particles and antiparticles with different quantum numbers grows exponentially with the amount of particles. Consequently, it is very challenging both analytically as well as numerically to predict the probability to which particular states will be finally occupied.

During electron-positron pair creation by strong electromagnetic fields, the initial vacuum state $\|\text{vac}\rangle\rangle$ evolves into a general Fock state $\|\Omega(t)\rangle\rangle$, which is a superposition of the vacuum state and several multipair states, each containing a specific number of pairs of particles and antiparticles. These multipair states are characterized by a set of various quantum numbers, e. g., the kinematic momentum \mathbf{p} and the spin $s = \pm\hbar/2$. In the Schrödinger picture, the quantum field state consisting of particle-antiparticle multipairs can be written as

of a discretized Hamiltonian) over the electronic annihilation operators and the positronic creation operators,

$$\hat{\Psi}(\mathbf{r}) = \sum_{p,s} \hat{a}_{p,s}^+ \psi_{p,s}^+(\mathbf{r}) + \sum_{p,s} \hat{a}_{p,s}^- \psi_{p,s}^-(\mathbf{r}). \quad (4)$$

Here, $\psi_{p,s}^+(\mathbf{r})$ denotes a normalized eigenstate of the free Dirac equation with positive energy, the momentum eigenvalue \mathbf{p} , and the spin s , and correspondingly $\psi_{p,s}^-(\mathbf{r})$ denotes an eigenstate with negative energy. This means, $\psi_{p,s}^+(\mathbf{r})$ and $\psi_{p,s}^-(\mathbf{r})$ are eigenfunctions of the first-quantization Dirac Hamiltonian

$$\hat{H}_D = c\boldsymbol{\alpha} \cdot (\hat{\mathbf{p}} - q\mathbf{A}(\mathbf{r}, t)) + \beta m_e c^2 + q\phi(\mathbf{r}, t) \quad (5)$$

in the special case of a vanishing electric potential $\phi(\mathbf{r}, t)$ and a vanishing magnetic vector potential $\mathbf{A}(\mathbf{r}, t)$. Here, we also introduced the momentum operator $\hat{\mathbf{p}}$, the electron’s charge $q = -e$, as well as the Dirac matrices $\boldsymbol{\alpha} = (\alpha_1, \alpha_2, \alpha_3)^T$ and β . Adopting the Heisenberg picture, the operators $\hat{\Psi}(\mathbf{r})$ and $\hat{a}_{p,s}^\pm$ become time dependent. The time-dependent field operator $\hat{\Psi}(\mathbf{r}, t)$ is given in terms of time-dependent creation and annihilation operators by

$$\hat{\Psi}(\mathbf{r}, t) = \sum_{p,s} \hat{a}_{p,s}^+(t) \psi_{p,s}^+(\mathbf{r}) + \sum_{p,s} \hat{a}_{p,s}^-(t) \psi_{p,s}^-(\mathbf{r}). \quad (6)$$

Stripping the antiparticle part from the quantum field operator (6), we define the operator [26]

$$\hat{\Psi}^+(\mathbf{r}, t) = \sum_{p,s} \hat{a}_{p,s}^+(t) \psi_{p,s}^+(\mathbf{r}). \quad (7)$$

With this definition operators representing various physical observables can be established, e. g., the generalized particle-number density operators

$$\hat{N}_n(t) = \frac{1}{n!} \hat{\Psi}^\dagger(\mathbf{r}_1, t) \hat{\Psi}^\dagger(\mathbf{r}_2, t) \cdots \hat{\Psi}^\dagger(\mathbf{r}_n, t) \hat{\Psi}(\mathbf{r}_1, t) \cdots \hat{\Psi}(\mathbf{r}_n, t) \quad (8)$$

can be introduced for $n = 1, 2, \dots$. The average density $\varrho(\mathbf{r}_1, \dots, \mathbf{r}_n, t)$ of finding simultaneously particles at the positions $\mathbf{r}_1, \dots, \mathbf{r}_n$ at time t if the system was initially in the quantum field state $|\Omega\rangle$ is given by

$$\varrho(\mathbf{r}_1, \dots, \mathbf{r}_n, t) = \langle\langle \Omega | \hat{N}_n(t) | \Omega \rangle\rangle. \quad (9)$$

Integrating over the whole space leads to the expectation values of the generalized particle number operators,

$$N_n(t) = \int \cdots \int \varrho(\mathbf{r}_1, \dots, \mathbf{r}_n, t) d^3r_1 \cdots d^3r_n. \quad (10)$$

The quantity $N_1(t)$ denotes the average number of particles at time t . In general, $N_n(t)$ is the average number of n -tuples of particles present at time t . These n -tuples may originate from a number state with n particles or from some state containing $m > n$ particles. In the special case that the initial state $|\Omega\rangle$ has evolved into a single number state of m pairs then $N_n(t) = \binom{m}{n}$ because there are $\binom{m}{n}$ ways to pick n particles from a set of m particles. This can also be confirmed by an explicit calculation of $N_n(t)$ for some m -particle state. Consequently, we can also write

$$N_n(t) = \sum_{m=n}^{\infty} \binom{m}{n} C_m(t), \quad (11)$$

where $C_m(t)$ denotes the total probability that $|\Omega\rangle$ has evolved into some number state with m pairs. This means with respect to the expansion coefficients $c_{n,m}$ of a quantum field state in the Schrödinger picture as in Eq. (1)

$$C_n(t) = \sum_m |c_{n,m}(t)|^2. \quad (12)$$

The set of linear equations (11) can be inverted to yield [27, 28]

$$C_n(t) = \sum_{m=n}^{\infty} (-1)^{m+n} \binom{m}{n} N_m(t). \quad (13)$$

The $C_n(t)$ characterize how many particle-antiparticle pairs are created preferably by the external strong electromagnetic fields. In analogy to the n -pair probability $C_n(t)$ as given in Eq. (13), we find the n -pair probability density

$$\begin{aligned} \rho(\mathbf{r}_1, \dots, \mathbf{r}_n, t) = \\ \sum_{m=n}^{\infty} (-1)^{m+n} \binom{m}{n} \int \cdots \int \varrho(\mathbf{r}_1, \dots, \mathbf{r}_m, t) d^3r_{n+1} \cdots d^3r_m. \end{aligned} \quad (14)$$

Here, position variables $\mathbf{r}_{n+1}, \dots, \mathbf{r}_m$ are integrated out. The choice of the integration variables, however, is of no relevance as the density $\rho(\mathbf{r}_1, \dots, \mathbf{r}_m, t)$ is invariant under permutation

of the position variables. Note that if the quantum field state is a superposition of n -pair states only, i. e., $C_n(t) = 1$, then $\rho(\mathbf{r}_1, \dots, \mathbf{r}_n, t) = \varrho(\mathbf{r}_1, \dots, \mathbf{r}_n, t)$.

To determine the densities defined in Eq. (9) and the expectation values (10) and (13), which are of main interest here, we need to solve the time dependence of the quantum field operator. The time-dependent quantum field operators as well as the creation and the annihilation operators fulfill the Heisenberg equations of motion

$$i\hbar \frac{\partial \hat{\Psi}(\mathbf{r}, t)}{\partial t} = [\hat{\Psi}(\mathbf{r}, t), \hat{H}] \quad (15)$$

and

$$i\hbar \frac{\partial \hat{a}_{p,s}^\pm(t)}{\partial t} = [\hat{a}_{p,s}^\pm(t), \hat{H}], \quad (16)$$

respectively, with the Hamilton operator

$$\hat{H} = \int \hat{\Psi}^\dagger(\mathbf{r}, t) \hat{H}_D \hat{\Psi}(\mathbf{r}, t) d^3r. \quad (17)$$

The equation of motion (15) can be further simplified via Eq. (17) to the Schrödinger-like equation [29]

$$i\hbar \frac{\partial \hat{\Psi}(\mathbf{r}, t)}{\partial t} = \hat{H}_D \hat{\Psi}(\mathbf{r}, t). \quad (18)$$

Consequently, the time-dependent field operator $\hat{\Psi}(\mathbf{r}, t)$ can also be expressed as

$$\hat{\Psi}(\mathbf{r}, t) = \sum_{p,s} \hat{a}_{p,s}^+ \psi_{p,s}^+(\mathbf{r}, t) + \sum_{p,s} \hat{a}_{p,s}^- \psi_{p,s}^-(\mathbf{r}, t), \quad (19)$$

where the functions $\psi_{p,s}^+(\mathbf{r}, t)$ and $\psi_{p,s}^-(\mathbf{r}, t)$ denote the solutions of the time-dependent Dirac equation with $\psi_{p,s}^+(\mathbf{r})$ and $\psi_{p,s}^-(\mathbf{r})$, respectively, as initial conditions at time $t = 0$ and with $\hat{a}_{p,s}^+ = \hat{a}_{p,s}^+(0)$ and $\hat{a}_{p,s}^- = \hat{a}_{p,s}^-(0)$. Equating Eqs. (6) and (19), we can solve for $\hat{a}_{p,s}^+(t)$ and $\hat{a}_{p,s}^-(t)$ and finally find [30, 31]

$$\hat{a}_{p,s}^+(t) = \sum_{p',s'} G(+|+)_{p,s;p',s'} \hat{a}_{p',s'}^+ + G(+|-)_{p,s;p',s'} \hat{a}_{p',s'}^- \quad (20)$$

and

$$\hat{a}_{p,s}^-(t) = \sum_{p',s'} G(-|+)_{p,s;p',s'} \hat{a}_{p',s'}^- + G(-|-)_{p,s;p',s'} \hat{a}_{p',s'}^+ \quad (21)$$

with the transition amplitudes

$$G(\nu|\nu')_{p,s;p',s'} = \langle \psi_{p',s'}^{\nu'}(\mathbf{r}) | \psi_{p,s}^\nu(\mathbf{r}, t) \rangle. \quad (22)$$

Assuming that initially the pure vacuum state $|\Omega\rangle = |\text{vac}\rangle$ is given, the density $\varrho(\mathbf{r}_1, \dots, \mathbf{r}_n, t)$ can be written by employing Eq. (3) and $\hat{a}_{p,s}^\pm |\text{vac}\rangle = 0$ and introducing the Hermitian matrix

$$S_{p,s;p',s'}(t) = \sum_{p'',s''} G(+|-)_{p,s;p'',s''}^* G(+|-)_{p'',s'';p',s'} \quad (23)$$

as

$$\varrho(\mathbf{r}_1, \dots, \mathbf{r}_n, t) = \frac{1}{n!} \sum_{\substack{\mathbf{p}_1, \mathbf{p}_2, \dots, \mathbf{p}_n \\ s_1, s_2, \dots, s_n \\ \mathbf{p}'_1, \mathbf{p}'_2, \dots, \mathbf{p}'_n \\ s'_1, s'_2, \dots, s'_n}} \left(\sum_{(i_1, i_2, \dots, i_n) \in P_n} \sigma_{i_1, i_2, \dots, i_n} S_{\mathbf{p}_1, s_1; \mathbf{p}'_1, s'_1}(t) S_{\mathbf{p}_2, s_2; \mathbf{p}'_2, s'_2}(t) \dots S_{\mathbf{p}_n, s_n; \mathbf{p}'_n, s'_n}(t) \right) \\ \times \psi_{\mathbf{p}_1, s_1}^+(\mathbf{r}_1)^\dagger \psi_{\mathbf{p}_2, s_2}^+(\mathbf{r}_2)^\dagger \dots \psi_{\mathbf{p}_n, s_n}^+(\mathbf{r}_n)^\dagger \psi_{\mathbf{p}'_1, s'_1}^+(\mathbf{r}_1) \dots \psi_{\mathbf{p}'_2, s'_2}^+(\mathbf{r}_2) \psi_{\mathbf{p}'_1, s'_1}^+(\mathbf{r}_1), \quad (24)$$

where the innermost sum runs over all permutations (i_1, i_2, \dots, i_n) of the set of the natural numbers 1 to n and $\sigma_{i_1, i_2, \dots, i_n}$ denotes the permutation's sign. Integrating (24) over the whole space, one gets

$$N_n(t) = \frac{1}{n!} \sum_{\substack{\mathbf{p}_1, \mathbf{p}_2, \dots, \mathbf{p}_n \\ s_1, s_2, \dots, s_n}} \sum_{(i_1, i_2, \dots, i_n) \in P_n} \sigma_{i_1, i_2, \dots, i_n} S_{\mathbf{p}_1, s_1; \mathbf{p}_{i_1}, s_{i_1}}(t) S_{\mathbf{p}_2, s_2; \mathbf{p}_{i_2}, s_{i_2}}(t) \dots S_{\mathbf{p}_n, s_n; \mathbf{p}_{i_n}, s_{i_n}}(t). \quad (25)$$

Note that the innermost sums in (24) and (25) represent a determinant. The outer sum over momenta and spins in (24) contains for each summand also its complex conjugate, thus $\varrho(\mathbf{r}_1, \dots, \mathbf{r}_n, t)$ is real valued. Furthermore, the outer sum over momenta and spins in (25) runs over determinants of Hermitian matrices, thus also $N_n(t)$ is real valued. For $n = 1$ and $n = 2$, Eqs. (24) and (25) simplify to

$$\varrho(\mathbf{r}_1, t) = \sum_{\substack{\mathbf{p}_1, s_1 \\ \mathbf{p}'_1, s'_1}} S_{\mathbf{p}_1, s_1; \mathbf{p}'_1, s'_1}(t) \psi_{\mathbf{p}_1, s_1}^+(\mathbf{r}_1)^\dagger \psi_{\mathbf{p}'_1, s'_1}^+(\mathbf{r}_1), \quad (26a)$$

$$\varrho(\mathbf{r}_1, \mathbf{r}_2, t) = \frac{1}{2} \sum_{\substack{\mathbf{p}_1, \mathbf{p}_2, s_1, s_2 \\ \mathbf{p}'_1, \mathbf{p}'_2, s'_1, s'_2}} \left(S_{\mathbf{p}_1, s_1; \mathbf{p}'_1, s'_1}(t) S_{\mathbf{p}_2, s_2; \mathbf{p}'_2, s'_2}(t) - S_{\mathbf{p}_1, s_1; \mathbf{p}'_2, s'_2}(t) S_{\mathbf{p}_2, s_2; \mathbf{p}'_1, s'_1}(t) \right) \psi_{\mathbf{p}_1, s_1}^+(\mathbf{r}_1)^\dagger \psi_{\mathbf{p}_2, s_2}^+(\mathbf{r}_2)^\dagger \psi_{\mathbf{p}'_2, s'_2}^+(\mathbf{r}_2) \psi_{\mathbf{p}'_1, s'_1}^+(\mathbf{r}_1), \quad (26b)$$

and

$$N_1(t) = \sum_{\mathbf{p}_1, s_1} S_{\mathbf{p}_1, s_1; \mathbf{p}_1, s_1}(t), \quad (27a)$$

$$N_2(t) = \frac{1}{2} \sum_{\mathbf{p}_1, s_1, \mathbf{p}_2, s_2} \left(S_{\mathbf{p}_1, s_1; \mathbf{p}_1, s_1}(t) S_{\mathbf{p}_2, s_2; \mathbf{p}_2, s_2}(t) - S_{\mathbf{p}_1, s_1; \mathbf{p}_2, s_2}(t) S_{\mathbf{p}_2, s_2; \mathbf{p}_1, s_1}(t) \right). \quad (27b)$$

Similarly to the position-space distribution $\varrho(\mathbf{r}_1, \dots, \mathbf{r}_n, t)$ one can introduce a momentum-space distribution $\chi_n(\mathbf{p}_1, \dots, \mathbf{p}_n, t)$ of the created particles, which reads

$$\chi_n(\mathbf{p}_1, \dots, \mathbf{p}_n, t) = \frac{1}{n!} \sum_{s_1, s_2, \dots, s_n} \sum_{(i_1, i_2, \dots, i_n) \in P_n} \sigma_{i_1, i_2, \dots, i_n} S_{\mathbf{p}_1, s_1; \mathbf{p}_{i_1}, s_{i_1}}(t) S_{\mathbf{p}_2, s_2; \mathbf{p}_{i_2}, s_{i_2}}(t) \dots S_{\mathbf{p}_n, s_n; \mathbf{p}_{i_n}, s_{i_n}}(t). \quad (28)$$

Accordingly, the single-particle and double-particle distributions simplify to

$$\chi_1(\mathbf{p}_1, t) = \sum_{s_1} S_{\mathbf{p}_1, s_1; \mathbf{p}_1, s_1}(t), \quad (29a)$$

$$\chi_2(\mathbf{p}_1, \mathbf{p}_2, t) = \frac{1}{2} \sum_{s_1, s_2} \left(S_{\mathbf{p}_1, s_1; \mathbf{p}_1, s_1}(t) S_{\mathbf{p}_2, s_2; \mathbf{p}_2, s_2}(t) - S_{\mathbf{p}_1, s_1; \mathbf{p}_2, s_2}(t) S_{\mathbf{p}_2, s_2; \mathbf{p}_1, s_1}(t) \right). \quad (29b)$$

Note that densities and expectation values of particle numbers for the antiparticle part of the created pairs can be derived, too, analogously to the particle case as outlined above. For this purpose, one has to replace the operator (7) in the definition of the particle-number density operator (8) by

$$\hat{\Psi}^-(\mathbf{r}, t) = \sum_{\mathbf{p}, s} \hat{a}_{\mathbf{p}, s}^-(t)^\dagger \psi_{\mathbf{p}, s}^-(\mathbf{r}). \quad (30)$$

In particular, the momentum-space distribution $\chi_n^-(\mathbf{p}_1, \dots, \mathbf{p}_n, t)$ of the created antiparticles yields

$$\chi_n^-(\mathbf{p}_1, \mathbf{p}_2, \dots, \mathbf{p}_n, t) = \frac{1}{n!} \sum_{s_1, s_2, \dots, s_n} \sum_{(i_1, i_2, \dots, i_n) \in P_n} \sigma_{i_1, i_2, \dots, i_n} S_{\mathbf{p}_1, s_1; \mathbf{p}_{i_1}, s_{i_1}}^-(t) S_{\mathbf{p}_2, s_2; \mathbf{p}_{i_2}, s_{i_2}}^-(t) \dots S_{\mathbf{p}_n, s_n; \mathbf{p}_{i_n}, s_{i_n}}^-(t), \quad (31)$$

where the matrix $S_{\mathbf{p}, s; \mathbf{p}', s'}^-(t) = \sum_{\mathbf{p}'', s''} G(-|_+)_{\mathbf{p}, s; \mathbf{p}'', s''}^* G(-|_+)_{\mathbf{p}'', s''; \mathbf{p}', s'}$ has been introduced.

3. Controlling pair creation triggered by a strong localized potential

3.1. Energy spectrum of a strong localized potential

The Coulomb binding potential supports several electronic bound states and with increasing potential depth these bound states can dive into the negative-energy continuum [32]. These embedded states can be viewed as the supercritical quasibound states, which build up the connection between positive and negative energy levels and in this way trigger spontaneous pair creation. The essential physics of this process can be represented by a one-dimensional model system, which we will employ for the remainder of this article. Note that in one dimension the Dirac equation reduces to an equation for two-component wave function with no spin [33]. For numerical feasibility, we choose a localized scalar potential well of the form

$$q\phi(x, t) = V_0(S(x + D/2) - S(x - D/2))f(t) \quad (32)$$

instead of the long range Coulomb field. Here the parameter D is related to the spatial width of the well, which is formed by two smooth unit-step functions

$$S(x) = \frac{1}{2} \left(1 + \tanh \frac{x}{W} \right), \quad (33)$$

where W is the extent of the associated localized electric fields [3]. The time-dependent function $f(t)$ describes the temporal profile of the external field. In our calculation, we employ

$$f(t) = \begin{cases} \sin^2 \frac{\pi(t-\Delta T)}{2\Delta T} & \text{for } -\Delta T \leq t \leq 0, \\ 1, & 0 \leq t \leq T \\ \cos^2 \frac{\pi(t-T)}{2\Delta T} & \text{for } T \leq t \leq T + \Delta T, \end{cases} \quad (34)$$

where T denotes the period of the flat plateau and ΔT the duration of turn-on and turn-off.

The field configuration at the plateau phase $0 \leq t \leq T$ can support several electronic bound states and as the potential height V_0 increases, the lower bound states can overlap with the negative-energy continuum. The resulting degeneracy between the quasibound states and the negative-energy continuum leads in the case of a discretized Dirac Hamiltonian, as it is employed in our numerical calculations, to an increased density of states as shown in Fig. 1. By varying the potential strength V_0 (or its width W), we can control the number of supercritical quasibound states in the negative continuum. As each number state has some energy that is at least $2m_e c^2$ times the number of pairs, it is commonly believed that single-pair states are preferably created over states consisting of several pairs. However, we will show in the following that if there is more than one supercritical quasibound state in the Dirac sea, the system will prefer to populate multipair states rather than single-pair states, which can be strongly suppressed.

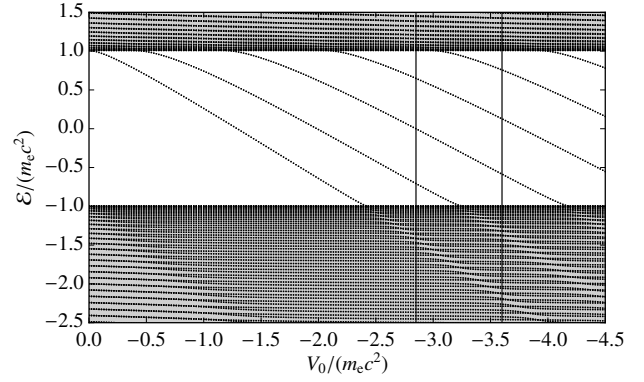


Figure 1: Energy eigenvalues \mathcal{E} of the discretized one-dimensional Dirac Hamiltonian with the potential (32) with $W = 0.3\lambda_C$ and $D = 3.2\lambda_C$ as a function of the potential strength V_0 with λ_C denoting the Compton wavelength. Gray shaded areas indicate the continuous spectrum of the underlying Dirac Hamiltonian \hat{H}_D . For the discretization of the Dirac Hamiltonian a regular spatial grid running from $-34.25\lambda_C$ to $34.25\lambda_C$ with 512 grid points was applied. The two vertical lines indicate the potential strengths that are employed in Figs. 2(a) and 2(b).

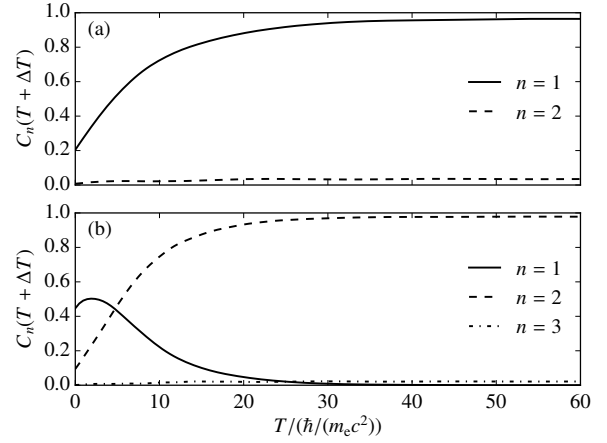


Figure 2: n -pair probabilities C_n as a function of the interaction time T after the potential has been smoothly turned off with $\Delta T = 4.7\hbar/(m_e c^2)$ for $V_0 = -2.85m_e c^2$ in (a) and $V_0 = -3.6m_e c^2$ in (b). Other parameters are as in Fig. 1.

3.2. Number states in pair creation

Figure 2 presents the probability C_n to create a number state of n pairs as a function of the interaction time T after the potential has been smoothly turned off at time $T + \Delta T$. In Fig. 2(a) with $V_0 = -2.85m_e c^2$, the quantum field state evolves into a superposition of single-pair states as $C_1(T + \Delta T) \approx 1$ for sufficiently long interaction times. There is only a small probability to populate two-pair states. The quantities $C_n(T + \Delta T)$ for $n > 2$ are so small that they cannot be distinguished from zero on the scale of Fig. 2 and are therefore not shown. As further numerical simulations show, the nonzero probability $C_2(T + \Delta T)$ results from the nonadiabatic turn-on and turn-off

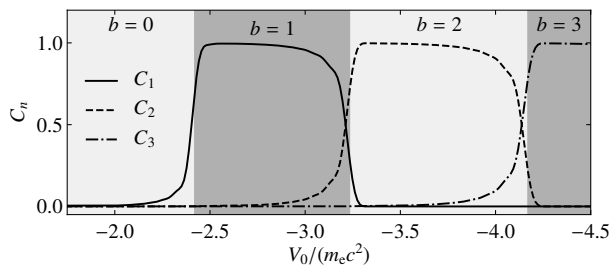


Figure 3: n -pair probabilities C_n as a function of the maximal potential strength V_0 after the potential has been smoothly turned off with a total interaction time $T = 93\hbar/(m_e c^2)$. Other parameters are as in Fig. 2. The gray shaded areas indicate parameter regions with a particular number of supercritical quasibound states b .

and can be reduced by switching the potential on and off more slowly. Apparently the creation of sole single-pair states is related to the fact that exactly one quasibound state in the negative continuum is present for the chosen potential parameters. Increasing the depth of the potential to $V_0 = -3.6m_e c^2$ creates a second quasibound state as indicated in Fig. 1. The n -pair probabilities C_n for this setup are presented in Fig. 2(b). For short interaction times we find a superposition of single-, two-, and three-pair states. Similar to the former case the nonzero probability $C_3(T + \Delta T)$ results from the nonadiabatic turn-on and turn-off. More interestingly, the single-pair states present for short interaction times disappear after some transient interval of interaction times T and for sufficiently long interaction times the quantum field state is almost only a superposition of two-pair states, i. e., $C_2(T + \Delta T) \approx 1$.

Our numerical results indicate that the number of the potential's quasibound states determines into what kind of number state the quantum field state evolves for sufficiently long interaction times. This is also illustrated in Fig. 3, where the probability C_n to create a number state of n pairs is shown as a function of the maximal potential strength V_0 and as a function of the number of supercritical quasibound states b . For potential parameters with b supercritical quasibound states we find $C_b \approx 1$, except for parameters close to a change of the value of b . This means one can control into which particle-number state the system will eventually evolve just by changing the number of supercritical quasibound states in the system. At least in principle, this number can be easily adjusted by varying the strength and the shape of the supercritical electric potential as the only two relevant parameters.

The supercritical quasibound states are commonly interpreted as different channels for pair creation. As shown in Refs. [20, 34], the complex scaling method can be utilized to determine the asymptotic pair-creation rate for each channel. As a (rather unexpected) central result, there is no competition between the different pair-creation channels, i. e., the number of created particles follows a *single* exponential law with a rate given by the sum of rates of the individual channels. Our results provide an intuitive explanation of this phenomenon. The presence of n quasibound states favors the population of multipair states; this means the *simultaneous* creation of n

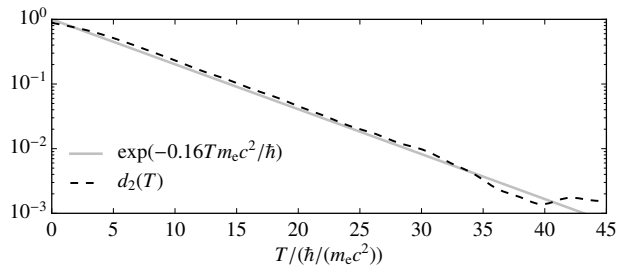


Figure 4: Decay probability d_2 as a function of the interaction time T after the potential has been smoothly turned off (dashed black line) and an exponential fit to the data (solid gray line). The potential height is $V_0 = -3.6m_e c^2$ and other parameters are as in Fig. 1.

particle-antiparticle pairs. In other words, the n supercritical quasibound states actually represent a single channel to create number states with n electron-positron pairs. To provide a more quantitative analysis, we define the quantity

$$d_n(T) = |C_n(T \rightarrow \infty) - C_n(T)|. \quad (35)$$

It characterizes how the initial vacuum state decays into a certain number state that is occupied with probability $C_n(T \rightarrow \infty)$ for an asymptotically long interaction time T . The quantity $d_2(T)$ corresponding to the decay of the vacuum state into two-pair states is shown on a logarithmic scale in Fig. 4. It follows approximately a straight line, which indicates that the decay process is exponential, namely $d_2(T) \sim \exp(-\gamma T)$ with the exponential parameter $\gamma \approx 0.16m_e c^2/\hbar$. According to Ref. [20], the exponential decay rate of the occupation of the particle-number state to its asymptotic value, which results from the complex scaling approach, is $\gamma \approx 0.18m_e c^2/\hbar$ for the same field configuration as in Figs. 2(b) and 4. The small discrepancy between these two exponents may be attributed to the occurrence of the intermediate single-particle states seen in Fig. 2(b), which slows down the transition from the vacuum into the final two-particle states.

3.3. Position- and momentum-space distributions

Our numerical space- and time-resolved analysis of the pair-creation dynamics allows us not only to determine how many particles and antiparticles are created but also where these are created. Figure 5 shows the asymptotic single- and two-particle probability densities $\varrho(x_1)$ and $\varrho(x_1, x_2)$ for the position of the electrons as calculated for the parameters as employed before and a potential strength of $V_0 = -2.85m_e c^2$ and $V_0 = -3.6m_e c^2$, i. e., where the final quantum field state consists asymptotically mainly of single-pair states and two-pair states, respectively, as discussed above. The single-particle densities are concentrated in the vicinity of the localized potential (32) for both cases. However, the origins of these distributions are different. For the case $V_0 = -2.85m_e c^2$, $\varrho(x_1)$ reflects the single-pair states, which are the dominating states for this potential strength. Furthermore, the two-particle density $\varrho(x_1, x_2)$ is close to zero

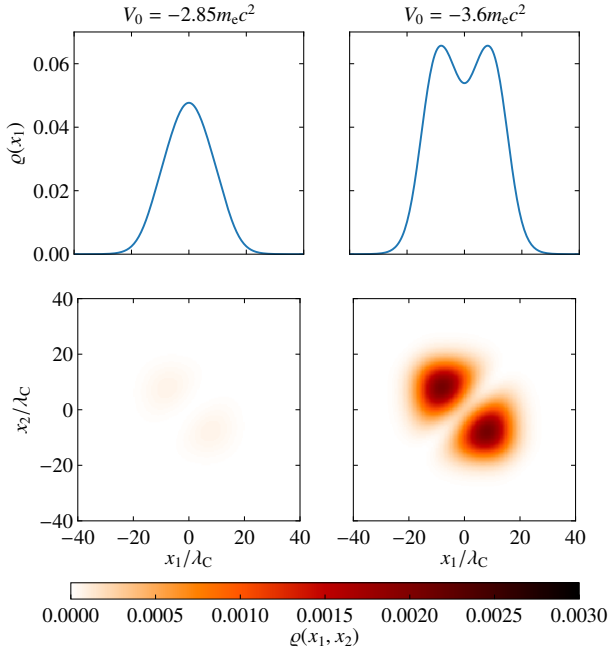


Figure 5: Single- and two-pair spatial densities $\rho(x_1)$ and $\rho(x_1, x_2)$ as calculated for the parameters as in Fig. 2 and a total interaction time $T = 90\hbar/(m_e c^2)$. The left column corresponds to a potential strength of $V_0 = -2.85m_e c^2$ and the right one is for $V_0 = -3.6m_e c^2$.

for $V_0 = -2.85m_e c^2$. For $V_0 = -3.6m_e c^2$ the two-pair states are the dominating states and single-pair states are not occupied as we mentioned before. Consequently, the two-particle density $\rho(x_1, x_2)$ is substantial in this case. It has two maxima at $(x_1, x_2) \approx (-7\lambda_C, 7\lambda_C)$ and $(x_1, x_2) \approx (7\lambda_C, -7\lambda_C)$. The single-particle density $\rho(x_1)$ is just the marginal distribution of $\rho(x_1, x_2)$ as there are no single-pair contributions to $\rho(x_1)$. As a consequence of the fermionic nature of the created particles and the Pauli exclusion principle, the density $\rho(x_1, x_2)$ vanishes along the line $x_1 = x_2$. Furthermore, the two created electrons that emerge at $\pm 7\lambda_C$ are strongly correlated, i. e., the spatial distributions of the two electrons are not statistically independent.

To complete our understanding of the decay process of the vacuum into multiple electron-positron pairs, we also investigate the properties of the created electrons and positrons in momentum space. The positrons are best characterized by its momentum spectrum, because for the positrons the localized potential is repulsive leading to a strong acceleration and delocalization. In contrast, the electrons are captured in the potential. This means the momentum distribution of the created electrons $\chi(p_1)$ is concentrated around zero as shown in Fig. 6. Due to the narrow potential and the resulting strong localization of the created electrons, the electrons' momentum distribution is rather broad, i. e., it has a width of the order of $m_e c$. The momentum distribution of the positrons $\chi^-(p_1)$ exhibits two peaks at $p_1 \approx \pm 1.01m_e c$ for the parameter $V_0 = -2.85m_e c^2$, as presented in Fig. 7. This means that the individual positrons, which emerge for this parameter set, travel with relativistic velocities to the left or to the right with

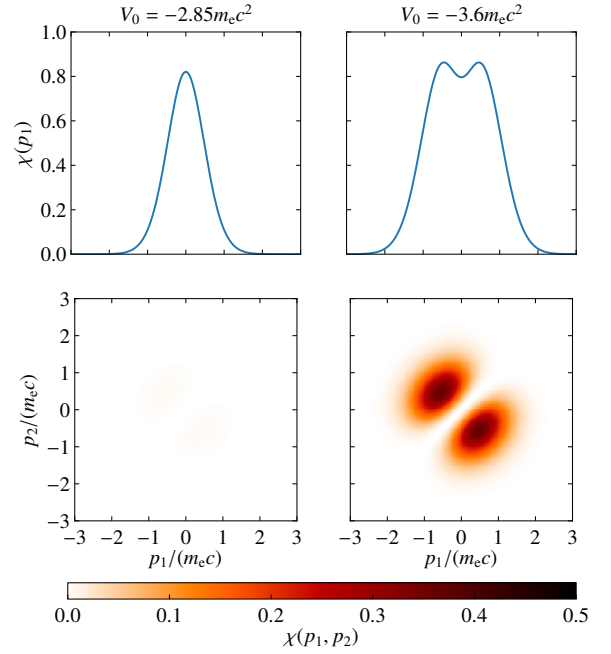


Figure 6: Single- and two-pair momentum spectra $\chi(p_1)$ and $\chi(p_1, p_2)$ of the created electrons as calculated for the parameters as in Fig. 2 and a total interaction time $T = 50\hbar/(m_e c^2)$. The left column corresponds to a potential strength of $V_0 = -2.85m_e c^2$ and the right one is for $V_0 = -3.6m_e c^2$.

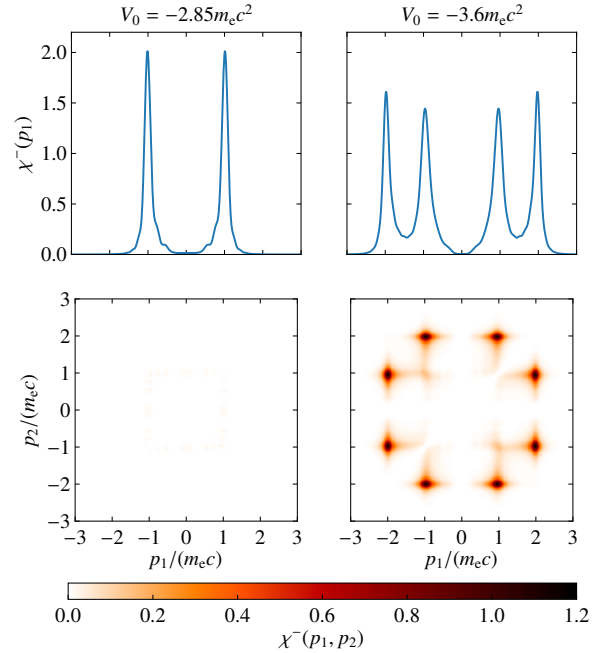


Figure 7: Single- and two-pair momentum spectra $\chi^-(p_1)$ and $\chi^-(p_1, p_2)$ of the created positrons as calculated for the parameters as in Fig. 2 and a total interaction time $T = 50\hbar/(m_e c^2)$. The left column corresponds to a potential strength of $V_0 = -2.85m_e c^2$ and the right one is for $V_0 = -3.6m_e c^2$.

equal probability. The distributions $\chi(p_1, p_2)$ and $\chi^-(p_1, p_2)$ almost vanish for $V_0 = -2.85m_e c^2$ as also indicated in Figs. 6 and 7, which again proves that single-pair states dominate the pair-creation process in this case. For $V_0 = -3.6m_e c^2$, the creation process is triggered by two different channels leading to an occupation of two-pair states and to a rich structure of the asymptotic positron momentum distribution $\chi^-(p_1, p_2)$. This distribution features eight sharp maxima approximately at $\pm 0.96m_e c$ and $\pm 1.98m_e c$. As there are no single-pair states for $V_0 = -3.6m_e c^2$, there are no single-pair contributions to the momentum distributions $\chi(p_1, t)$ and $\chi^-(p_1, t)$ which therefore follow from $\chi(p_1, p_2)$ and $\chi^-(p_1, p_2)$, respectively, by integrating out one momentum degree. Because of the Pauli exclusion principle for indistinguishable fermions, the corresponding two electrons/positrons cannot have the same momentum and, therefore, the distributions $\chi(p_1, p_2)$ and $\chi^-(p_1, p_2)$ vanish along the line $p_1 = p_2$.

Signatures of the supercritical quasibound states are observable also in the energy spectrum of the created electrons and positrons. Most likely, the created electrons have close-to-zero momentum, thus their energy distribution is sharply peaked at $m_e c^2$. Furthermore, the energy of the created positrons equals approximately the absolute value of the energy of the supercritical quasibound states. For $V_0 = -2.85m_e c^2$, for example, the individual positrons of the single-pair states travel with relativistic velocities to the left or right with equal probability having a total energy of about $1.4m_e c^2$, which equals the absolute value of the energy of the supercritical quasibound state for this potential strength; see Fig. 1. For $V_0 = -3.6m_e c^2$, the energies that correspond to the positions of maxima in the momentum distribution of Fig. 7 are $1.39m_e c^2$ and $2.22m_e c^2$, which agree again with the energy values of the supercritical quasibound states in Fig. 1. Consequently, the net energy of the created particles equals approximately the energy gap between the energies of the supercritical quasibound states and the rest-mass energy of a real particle, i. e., $m_e c^2$.

4. Conclusions

In this work, we applied a time- and space-resolved formulation of quantum field theory to study fermionic strong-field pair cre-

ation. The theoretical foundation of this framework is based on the observation that the quantum field theoretical state can be directly related to the evolution of the time-dependent field operator in the Heisenberg picture. The evolution of the latter can be obtained from the dynamics of single-particle states of the Dirac Hamiltonian. This approach provides access to the full quantum field states and to expectation values of any physical observable for arbitrary external field configuration, e. g., the probability to create a certain number of electron-positron pairs. The Coulomb binding energy can become supercritical, i. e., quasibound states embedded in the negative-energy continuum initiate pair creation from the vacuum. For bosonic systems, it was demonstrated in Ref. [35] that the energy spectrum of the corresponding single-particle Hamiltonian determines the dynamics of the pair-creation process. Here, we studied the relation between the energy spectrum and pair creation for fermionic systems.

As a main result, we showed that the number of quasibound states of the Dirac Hamiltonian at maximal potential strength equals the number of created electron-positron pairs for a sufficiently long interaction time. This means that the pair-creation dynamics populates selectively multipair states with a specific number of electron-positron pairs. Consequently, one can control the number of created pairs by varying the applied potential such that it has a specific number of supercritical quasibound states. Furthermore, the sum of the mean energy of the created particles equals approximately the difference between the energy of the quasibound states and $m_e c^2$ summed over all quasibound states. As the applied localized potential is attractive for electrons their energy is close to their rest-mass energy, while positrons are accelerated to relativistic velocities. If there are several electrons/positrons created, they are strongly statistical dependent as a consequence of the Pauli exclusion principle.

Acknowledgments

This work was supported by the Alexander von Humboldt Foundation. Q. Z. Lv enjoyed several helpful discussions with Dr. Q. Su, Dr. R. Grobe, Dr. M. Jiang and Dr. Y. T. Li at the onset of this work.

-
- [1] A. Di Piazza, C. Müller, K. Z. Hatsagortsyan, and C. H. Keitel, *Rev. Mod. Phys.* **84**, 1177 (2012).
 - [2] W. Heisenberg and H. Euler, *Z. Phys.* **98**, 714 (1936).
 - [3] F. Sauter, *Z. Phys.* **69**, 742 (1931).
 - [4] J. Schwinger, *Phys. Rev.* **82**, 664 (1951).
 - [5] A. Hansen and F. Ravndal, *Phys. Scr.* **23**, 1036 (1981).
 - [6] B. R. Holstein, *Am. J. Phys.* **66**, 507 (1998).
 - [7] R. Schützhold, H. Gies, and G. Dunne, *Phys. Rev. Lett.* **101**, 130404 (2008).
 - [8] M. Ruf, G. R. Mocken, C. Müller, K. Z. Hatsagortsyan, and C. H. Keitel, *Phys. Rev. Lett.* **102**, 080402 (2009).
 - [9] S. S. Bulanov, V. D. Mur, N. B. Narozhny, J. Nees, and V. S. Popov, *Phys. Rev. Lett.* **104**, 220404 (2010).
 - [10] A. Wöllert, H. Bauke, and C. H. Keitel, *Phys. Rev. D* **91**, 125026 (2015).
 - [11] B. Müller, H. Peitz, J. Rafelski, and W. Greiner, *Phys. Rev. Lett.* **28**, 1235 (1972).
 - [12] M. Jiang, Q. Z. Lv, Z. M. Sheng, R. Grobe, and Q. Su, *Phys. Rev. A* **87**, 042503 (2013).
 - [13] F. Fillion-Gourdeau, E. Lorin, and A. D. Bandrauk, *Phys. Rev. Lett.* **110**, 013002 (2013).
 - [14] S. Tang, B.-S. Xie, D. Lu, H.-Y. Wang, L.-B. Fu, and J. Liu, *Phys. Rev. A* **88**, 012106 (2013).

- [15] T. Cowan, H. Backe, K. Bethge, H. Bokemeyer, H. Folger, J. S. Greenberg, K. Sakaguchi, D. Schwalm, J. Schweppe, K. E. Stiebing, and P. Vincent, *Phys. Rev. Lett.* **56**, 444 (1986).
- [16] I. Ahmad, S. M. Austin, B. B. Back, R. R. Betts, F. P. Calaprice, K. C. Chan, A. Chishti, C. Conner, R. W. Dunford, J. D. Fox, *et al.*, *Phys. Rev. Lett.* **78**, 618 (1997).
- [17] W. Greiner, B. Müller, and J. Rafelski, *Quantum Electrodynamics of Strong Fields*, Texts and Monographs in Physics (Springer, Berlin, 1985).
- [18] C. Brif, R. Chakrabarti, and H. Rabitz, *New J. Phys.* **12**, 075008 (2010).
- [19] P. Krekora, K. Cooley, Q. Su, and R. Grobe, *Phys. Rev. Lett.* **95**, 070403 (2005).
- [20] Q. Z. Lv, Y. Liu, Y. J. Li, R. Grobe, and Q. Su, *Phys. Rev. Lett.* **111**, 183204 (2013).
- [21] D. M. Gitman, *J. Phys. A: Math. Gen.* **10**, 2007 (1977).
- [22] V. P. Frolov and D. M. Gitman, *J. Phys. A: Math. Gen.* **11**, 1329 (1978).
- [23] E. S. Fradkin, D. M. Gitman, and S. M. Shvartsman, *Quantum Electrodynamics with Unstable Vacuum*, Springer Series in Nuclear and Particle Physics (Springer, Berlin, 1991).
- [24] A. Wöllert, H. Bauke, and C. H. Keitel, *Phys. Lett. B* **760**, 552 (2016).
- [25] Note that upper indices $+/-$ refer to the sign of the particles' energy as within the single-particle picture of the Dirac theory, not to the particles' charge.
- [26] S. S. Schweber, *An Introduction to Relativistic Quantum Field Theory*, Dover Books on Physics (Dover, Mineola, 2005).
- [27] T. Cheng, Q. Su, and R. Grobe, *Phys. Rev. A* **80**, 013410 (2009).
- [28] Q. Su, Y. T. Li, and R. Grobe, *Laser Phys.* **22**, 745 (2012).
- [29] W. Greiner and J. Reinhardt, *Field Quantization* (Springer, Berlin, 1996).
- [30] P. Krekora, Q. Su, and R. Grobe, *Phys. Rev. Lett.* **92**, 040406 (2004).
- [31] T. Cheng, Q. Su, and R. Grobe, *Contemp. Phys.* **51**, 315 (2010).
- [32] W. Greiner, *Relativistic Quantum Mechanics Wave Equations* (Springer, Berlin, 1997).
- [33] B. Thaller, *Advanced Visual Quantum Mechanics* (Springer, Berlin, Heidelberg, 2000).
- [34] Q. Z. Lv, Y. Liu, Y. J. Li, R. Grobe, and Q. Su, *Phys. Rev. A* **90**, 013405 (2014).
- [35] Q. Z. Lv, H. Bauke, Q. Su, C. H. Keitel, and R. Grobe, *Phys. Rev. A* **93**, 012119 (2016).